BNL-77772-2007-JA

Magnetization, RRR and Stability of Nb_3Sn Strands with High Sub-Element Number

L.D. Cooley, P.S. Chang, A.K. Ghosh

Accepted for Publication in IEEE Transaction on Applied Superconductivity (2007)

March 16, 2007

Superconducting Magnet Division

Brookhaven National Laboratory
P.O. Box 5000
Upton, NY 11973-5000
www.bnl.gov

Notice: This manuscript has been authored by employees of Brookhaven Science Associates, LLC under Contract No. DE-AC02-98CH10886 with the U.S. Department of Energy. The publisher by accepting the manuscript for publication acknowledges that the United States Government retains a non-exclusive, paid-up, irrevocable, world-wide license to publish or reproduce the published form of this manuscript, or allow others to do so, for United States Government purposes.

This preprint is intended for publication in a journal or proceedings. Since changes may be made before publication, it may not be cited or reproduced without the author's permission.

DISCLAIMER

This report was prepared as an account of work sponsored by an agency of the United States Government. Neither the United States Government nor any agency thereof, nor any of their employees, nor any of their contractors, subcontractors, or their employees, makes any warranty, express or implied, or assumes any legal liability or responsibility for the accuracy, completeness, or any third party's use or the results of such use of any information, apparatus, product, or process disclosed, or represents that its use would not infringe privately owned rights. Reference herein to any specific commercial product, process, or service by trade name, trademark, manufacturer, or otherwise, does not necessarily constitute or imply its endorsement, recommendation, or favoring by the United States Government or any agency thereof or its contractors or subcontractors. The views and opinions of authors expressed herein do not necessarily state or reflect those of the United States Government or any agency thereof.

Printed on recycled paper

Magnetization, RRR and Stability of Nb_3Sn Strands with High Sub-element Number

L. D. Cooley, P. S. Chang, and A. K. Ghosh

***Abstract*—The magnetization and low field stability were measured on a series of high current-density Nb_3Sn strands with 54 to 198 sub-elements taken from accelerator magnet development programs. The effective filament size, d_{eff}, as determined from the width of the magnetization loop at low field and the extrapolation of the transport critical current from high field, was very close to the sub-element diameter determined by the strand geometry. Self-field corrections were vital for obtaining this agreement; without them, d_{eff} was overestimated by ~25%. While all strands, even those with d_{eff} as small as 35 μm, exhibited flux-jumps at low field in magnetization measurements, smaller sub-elements produced smaller flux-jump magnitude and a smaller range of field over which flux jumps occurred, suggesting stability improved with decreasing d_{eff}. However, good combinations of the residual resistivity ratio *RRR* and the critical current density J_c became increasingly difficult to obtain by varying the reaction heat treatment as the sub-element number increased. Further analyses of *RRR* data indicate that tin contamination of the copper stabilizer is underway even before any Nb_3Sn is formed in strands with high numbers of sub-elements.**

***Index Terms*—Conductivity, Magnetic Field Measurement, Niobium Compounds, Stability, Superconducting Magnets**

I. Introduction

Niobium-tin superconducting strands are a core component of accelerator magnet research and development programs. Modern strand designs, such as the "restacked rod process" (RRP) strands considered in this paper from Oxford Instruments–Superconducting Technology [1],[2], attain very high critical current density J_c, now routinely about 3,000 A mm^{-2} in the non-copper area at 12 T field and 4.2 K temperature. To attain such high performance, copper is removed from the sub-element and replaced with Nb and Sn to the highest degree possible. This choice has a side-effect, namely the tendency for the Nb filaments to merge into a single Nb_3Sn mass during the reaction, which drives up the effective filament diameter d_{eff} to close to the sub-element diameter d_s.

Many wire designs, such as those considered in this paper, also use Nb diffusion barriers. In that case, to maximize the area fraction of the strand that is converted to Nb_3Sn and hence maximize the non-copper J_c, almost full reaction of the Nb diffusion barrier is also intended. This has 2 additional side-effects: (1) the barrier forms a continuous ring of superconducting Nb_3Sn, which makes $d_{eff} \approx d_s$ regardless of any filament merging; and (2) the front of diffusing tin is allowed to come dangerously close to the copper stabilizer, often resulting in contamination. These two effects combine in a particularly bad way for the magnet designer, because the large d_{eff} allows even the slightest disturbance to trigger a flux jump (especially at low fields where J_c and the stored magnetic energy in the strand is high), which releases heat that cannot escape due to the poor thermal conductivity of Cu-Sn [3]–[6].

A workaround for this situation has been developed recently [4]. By measuring the voltage for a constant applied current while sweeping the field, it is possible to experimentally determine the current density J_s at which low-field flux-jumps initiate quenches [5]. This stability threshold largely agrees with stability calculations and other observed quench behavior [6]. J_s falls with increasing final reaction time, and its fall is preceded in time by a drop in *RRR*, which we have suggested is evidence for a dynamic threshold related to heat transfer through tin-contaminated copper [4]. If the reaction parameters are chosen to optimize *both RRR* and J_c, then it is possible to maintain J_s comfortably above J_c, thus ensuring that the magnet load line never passes through a region of unstable operation.

Although it is possible to build working magnets with this paradigm, open questions remain about the effects of flux-jumps and their recovery on field quality and correction [7]. It is also desirable to simply improve the overall stability of Nb_3Sn strands, as well as reduce the field errors due to the superconductor magnetization. To this end, new conductors made under the U.S. High-Energy Physics (HEP) Conductor Development Program [8] have contained larger numbers of sub-elements to produce smaller d_s. The purpose of this paper is to analyze how reducing d_s affects the stability situation outlined above.

II. Experiment

The RRP strands examined in this study were drawn from inventories at Lawrence Berkeley National Laboratory and Brookhaven National Laboratory, using strands developed explicitly for the Conductor Development Program. The strands and their important parameters are listed in Table I. The sub-element designs are very similar for all of the strands except 8079, which had a lower tin fraction than the others. All

Manuscript received August 28, 2006. This work was supported by the U.S. Department of Energy under Contract DE-AC02-98CH10886.

L. D. Cooley and A. K. Ghosh are with Brookhaven National Laboratory, PO Box 5000, Upton, NY 11973 USA (e-mail: ldcooley@bnl.gov).

P. S. Chang is a student with the Materials Science Department, State University of New York at Stony Brook. He is supported by a NSF supplemental grant through the MRSEC for Thermal Spray Research.

TABLE I
SAMPLE PARAMETERS AND EXPERIMENTAL RESULTS

ID	Final HT	R	N	d_s (μm)	J_c (12T) (A mm^{-2})[a]	RRR	J_s (A mm^{-2})	J_M (3T) (kA mm^{-2})[a]	d_{eff} (μm)
7054-A	72 h @ 675 °C	1.00	54	67.4	2900	6	1880	19.4	69.5
7054-B	36 h @ 660 °C	1.00	54	67.4	2985	47	3560	18.4	62.5
7054-C	24 h @ 650 °C	1.00	54	67.4	2760	127	4650	--	--
7471-A	100 h @ 665 °C	0.92	54[b]	78.6	2290	6	1290	--	--
7471-B	50 h @ 665 °C	0.92	54[b]	78.6	2120	96	3560	15.2	28.9
8502-B	48 h @ 650 °C	0.79	84	57.1	3050	165	5580	20.8	57.2
8079-A	48 h @ 695 °C	0.70	90	56.6	2680	20	3190	--	--
8079-C	36 h @ 635 °C	0.70	90	56.6	2330	344	5290	17.5	49.3
8521-B	48 h @ 665 °C	0.91	108	48.7	2830	127	5580	--	--
7904-A	72 h @ 665 °C	0.68	126	48.1	2260	4	1320	--	--
7904-B	72 h @ 635 °C	0.68	126	48.1	2040	9	2310	18.1	45.8
7904-C	36 h @ 635 °C	0.68	126	48.1	1910	114	5280	--	--
8466-B	48 h @ 650 °C	0.85	198	36.6	2460	12	3783	19.5	38.3

All wires are 0.70 mm diameter except for 7471, which was 0.8 mm diameter.
[a]A self-field correction to the transport data was applied to the 3 T extrapolation but not to the 12 T extrapolation.
[b]Each sub-element contained 6 radial columns of Ta filaments to divide the Nb_3Sn area after reaction. The wire is similar to billet 7261 in [3].

strands were reacted on stainless steel barrels in a vacuum furnace, as we have described previously [9]. Also, the initial reaction stages were the same for all strands: 48 h @ 210 °C followed by 48 h @ 400 °C, with 50 °C h^{-1} ramp rates between soak stages. Because smaller sub-elements provide a shorter length over which tin must diffuse, different final reaction time/temperature combinations were used. These choices, also listed in Table I, were based both on the manufacturer's recommendations and on our past experience. They are separated into 3 categories appended to the billet ID: *aggressive* (A), which sought to maximize J_c; *balanced* (B), which sought to keep $RRR > 40$ while still providing high J_c; and *conservative* (C), which was very minimal. The choice of 635 and 665 °C temperatures is based on our empirical observation of approximately double reaction rate for every 15°C temperature rise in the vicinity of 650 °C.

After reserving one turn of each reacted strand for magnetization measurements, the transport critical current measurements followed procedures described previously [9]. An additional length of the strand was soldered in the transition region where the current transfers between the strand and copper current lead. A laser micrometer was used to measure the strand diameter d_w before reaction, and the copper to non-copper area ratio R was provided by the manufacturer. These were used to determine the non-copper area. Voltage-current (V-I) data were acquired in 0.5 T intervals from 8 T to the 11.5 T limit of our magnet to determine J_c (criterion: 10^{-14} Ω-m). This was followed by the acquisition of voltage-field (V-H) data for applied field $\mu_0 H$ from 0 to 4 T to determine J_s [5]. The product $J_c^{0.5}(\mu_0 H)^{0.25}$ produced data that could be fit by a line with a high degree of accuracy (least-squares quality factor > 0.999), which was used to make $J_c(\mu_0 H)$ extrapolations to the 12 T conductor benchmark field. J_c(12T) and J_s are summarized in Table I.

Magnetization measurements were conducted in a commercial SQUID magnetometer at 4.5 K looping between –3 to +5 T. These results are shown in Fig. 1. Short pieces of the strands, approximately 7 mm long and 15 to 20 mg mass, were mounted on nonmagnetic holders such that the field was perpendicular to the strand axis. The sample mass, the density of copper (8,980 kg m^{-3}), and the copper to non-copper area ratio were used to determine the total volume of the sub-elements and convert magnetic moment to magnetization M. The effective filament diameter was then calculated by inverting the critical state equation $J_M = 3\pi\Delta M\,(4d_{eff})^{-1}$, where ΔM is the full hysteresis at 3 T field and J_M is the value of the transport critical current density extrapolated to 3 T from the $J_c^{0.5}(\mu_0 H)^{0.25}$ product fit. A self-field correction was applied to the $J_c(\mu_0 H)$ data prior to the extrapolation, as discussed later. The J_M(3T) and d_{eff} values obtained are listed in Table I.

The sub-element diameter was estimated by using $d_s = d_w [N(1 + R)]^{-1/2}$, where N is the number of sub-elements. RRR was determined by measuring the ratio of strand resistance at room temperature and at the first onset of normal resistance for warming the strand above the helium bath (~20 K).

III. RESULTS AND DISCUSSION

A central question facing advanced Nb_3Sn conductor development is overcoming the instability issues outlined in the introduction. For many reasons, reducing the sub-element diameter should improve strand stability. Foremost, the reduction of the sub-element diameter should reduce the strand magnetization by the concomitant reduction of d_{eff}. This is indeed found. Fig. 1 shows that the magnetization hysteresis decreases as N increases. Since d_s is proportional to $N^{-1/2}$, the magnetization is thus decreasing as d_s decreases. It is noteworthy that billet 8466 achieves the HEP goal [8] of <40 μm d_{eff}. Also, there is progress toward reducing d_s without compromising performance, as indicated by the excellent results for billets 8502 and 8521.

However, it is not yet possible to eliminate flux-jumps altogether by restacking or dividing sub-elements [3]. Fig. 1 also shows that none of the strands tested were free from flux jumps. Together with the data in Table I, it can be seen that flux jumps are still present above ~0.5 T field even for d_{eff} < 30 μm. In V-H data, we often noticed that reproducible flux jumps would occur upon decreasing the field from a higher value at which the wire was stable. This suggests that the flux jumps in the first and fourth quadrants of $M(\mu_0 H)$ in Fig. 1 give an indication of the onset of instability. To analyze this

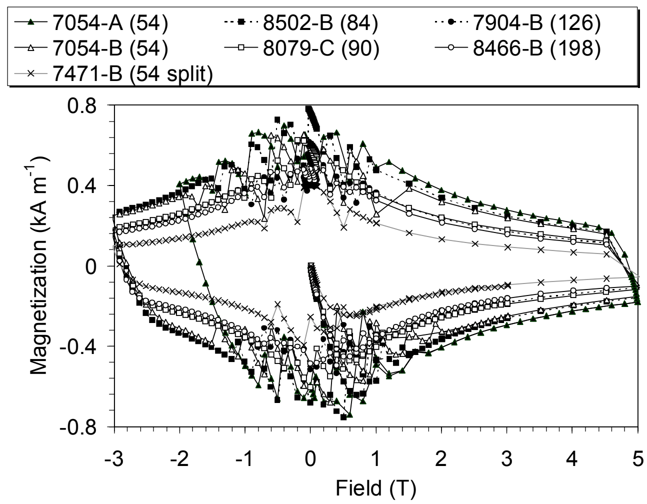

Fig. 1. Magnetization as a function of applied field. Decreases in hysteresis and in the onset field for flux jumps occur as the sub-element number (indicated at the top) increases. Much of the data for 7904-B overlaps the data for 8079-C and 8466-B.

further, in Fig. 2 the (decreasing) field at which such a flux jump occurs is plotted against d_{eff}. While these data suggest a generally lower flux-jump onset field with smaller d_{eff}, it is not possible to draw a trend line through these data to predict the effective filament diameter where flux jumps should cease altogether. Part of the problem is that J_c varies by ~30%, leading to significant scatter in M because $M \propto J_c d_{eff}$. For instance, the very conservative sample 8079-C displays the lowest onset field in Fig. 2 due to its weak critical current density.

The effective filament diameter obtained by comparing transport and magnetization data tracks closely with the predicted sub-element diameter based on the strand geometry. This is plotted in Fig. 3. However, large errors can occur when the transport J_c data is not corrected for self-field prior to extrapolating $J_c^{0.5}(\mu_0 H)^{0.25}$ to low field to obtain J_M. To emphasize this point, d_{eff} values calculated from extrapolating the uncorrected transport J_c are also shown, which are about 25% higher. These tendencies have been noted previously for Nb-Ti accelerator magnet strands [10], and their presence here verifies the high degree of uniformity of the sub-element cross-sections.

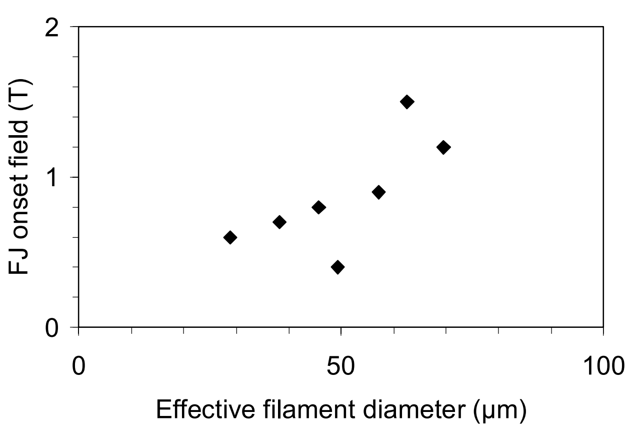

Fig. 2. The field at which flux jumps occur in the first and fourth quadrant of magnetization (Fig. 1), as a function of the effective filament diameter.

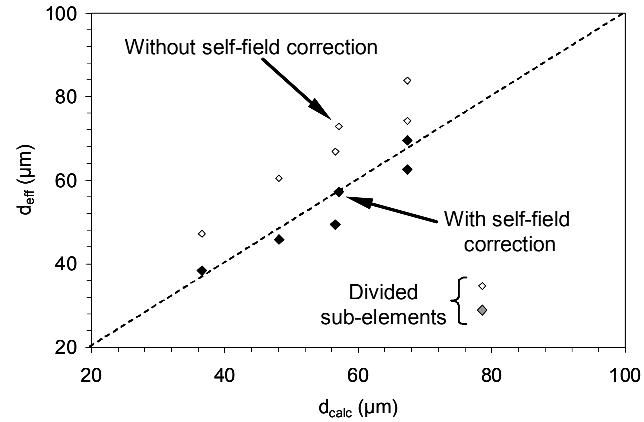

Fig. 3. The effective filament diameter is plotted as a function of the sub-element diameter calculated from d_w, N, and R. Filled symbols represent d_{eff} calculations using transport J_c data corrected for self-field, while open symbols represent similar calculations without the self-field correction. Results for billet 7471 with divided sub-elements are also indicated.

One data point in Fig. 3 shows that dividing the sub-element can be very useful for reducing the effective filament diameter. The data in Table I (billet 7471) indicates that a compromise of about 25% in performance is required, reducing J_c(12T) from ~3000 to ~2250 A mm^{-2}. This is due to the sub-element area devoted to the dividers. For comparison, Table I also indicates substantially higher J_c as well as good combinations of J_c and RRR are available without subdividing the sub-element (especially for billets 8502 and 8521) down to $d_s \approx 50$ μm. On the other hand, the J_c data generally display a downward trend with increasing N, suggesting that it becomes more difficult to maintain this performance as d_s is reduced below 40 μm. Thus, there does not seem to be a clear advantage for increasing N further vs. optimizing the divided-sub-element approach; both appear to be promising.

Since ductility is more difficult to maintain for larger numbers of restacked sub-elements, loss of conductor uniformity could be offsetting the advantage of utilizing the full sub-element area to form superconductor. In particular, thinning or rupture of the diffusion barrier presents a serious obstacle against heat treatment optimization. Although diffusion distances scale with d_s, a breach of the barrier would open the stabilizer up to contamination even before any Nb_3Sn is formed. This may explain why several entries in Table I have low RRR values when $N>108$. Indeed, some evidence for this problem is presented in Fig. 4, which shows a plot of the value of RRR obtained for strands extracted after the first two reaction stages (48 h @ 210°C + 48 h @ 400°C), but before the final stage, versus the number of sub-elements. Although all of the RRR values remain above 250, the ~30% drop as N increases from 54 to 198 suggests that trace contamination is already present in wires with high numbers of sub-elements. An alternative explanation of this trend is electron scattering by the subelements themselves, due to the thickness of the copper between the subelements becoming on the order of the electron mean free path at low temperatures for high N.

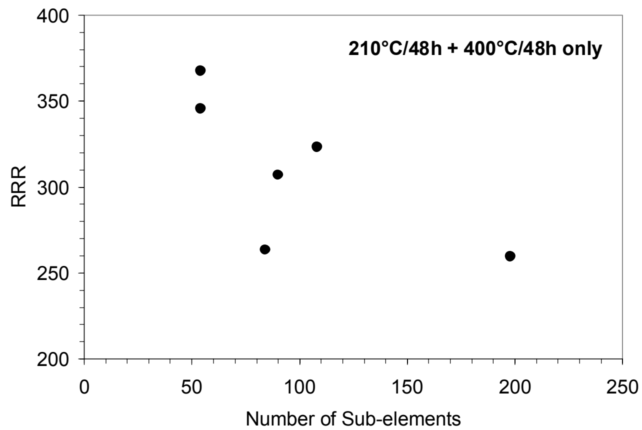

Fig. 4. The residual resistivity ratio is plotted as a function of the number of sub-elements for wire samples extracted prior to the high-temperature stage of the heat treatment, and thus prior to the expected formation of any Nb_3Sn.

IV. Conclusion

Significant progress has been made to reduce the strand magnetization, either by reducing the sub-element diameter or by dividing the sub-element. It is now possible to achieve ~3000 A mm^{-2} performance in strands with ~100 sub-elements, while also retaining *RRR* > 100 and reaching an effective filament diameter of just under 50 µm. Restacks of 198 sub-elements and strands with divided sub-elements both achieve still lower d_{eff}, but each displayed a significant loss of performance. No strand design examined in this paper produced magnetization curves that were free from flux jumps. Moreover, the data analysis could not predict a clear d_{eff} value at which flux jumps should disappear. For magnet designers, these trends suggest that significant progress still must be made before flux-jump instabilities are removed, which makes it essential to continue to optimize both J_c and *RRR*. Although tin diffusion distances are shorter in strands with smaller sub-elements, suggesting that reactions can be completed more quickly, evidence was given suggesting the start of tin contamination of the copper stabilizer even before any Nb_3Sn formed. This suggests that the two-parameter optimization above may be more difficult to attain for strands with smaller sub-elements.

Acknowledgment

We would like to thank J. Parrell, S. Hong, and M. Field for consultation on the RRP strands, and D. Dietderich (LBNL) for providing lengths of RRP strands from their inventory. E. Sperry and J. D'Ambra performed strand testing at BNL.

References

[1] S. Hong, M. B. Field, J. A. Parrell, and Y. Zhang, "Latest Improvements of Current Carrying Capability of Niobium Tin and Its Magnet Applications", *IEEE Trans. Appl. Supercond.*, Vol. 16, Issue 2, Pages 1146 – 1151, June 2006.

[2] J. A. Parrell, M. B. Field, Y. Zhang, and S. Hong, "Advances in Nb_3Sn strand for fusion and particle accelerator applications", *IEEE Trans. Appl. Supercond.*, Vol. 15, Issue 2, Part 2, Pages 1200 – 1204, June 2005.

[3] A. K. Ghosh, L. D. Cooley, A. R. Moodenbaugh, J. A. Parrell, M. B. Field, Y. Zhang, and S. Hong, "Magnetization studies of high J_c Nb_3Sn strands," *IEEE Trans. Appl. Supercond.*, vol. 15, no. 2, pp. 3494–3497, Jun. 2005.

[4] A. K. Ghosh, E. A. Sperry, L. D. Cooley, A. R. Moodenbaugh, R. L. Sabatini, and J. L. Wright, "Dynamic stability threshold in high-performance internal-tin Nb_3Sn superconductors for high field magnets", *Supercond. Sci. Technol.*, Vol. 18, No. 1, Pages L5 – L8, January 2005.

[5] A. K. Ghosh, L. D. Cooley, and A. R. Moodenbaugh, "Investigation of instability in high J_c Nb Sn strands," *IEEE Trans. Appl. Supercond.*, vol. 15, no. 2, pp. 3360–3363, Jun. 2005.

[6] E. Barzi, N. Andreev, B. Bordini, L. Del Frate, V. V. Kashikhin, D. Turrioni, R. Yamada, and A. V. Zlobin, "Instabilities in transport current measurements of Nb_3Sn strands," *IEEE Trans. Appl. Supercond.*, vol. 15, no. 2, pp. 3364–3367, Jun. 2005.

[7] S. Peggs, Brookhaven National Laboratory and LHC Accelerator Research Project, Upton, NY, private communication, April 2006.

[8] R. M. Scanlan and D. R. Dietderich, "Progress and plans for the U.S. HEP conductor development program" *IEEE Trans. Appl. Supercond.*, Vol. 13, Issue 2, Part 2, Pages 1536 – 1541, June 2003.

[9] R. Soika, L. D. Cooley, A. K. Ghosh, and A. Werner, "Fixture for short sample testing of modern high energy physics Nb_3Sn strands", *Adv. Cryo. Eng. (Materials)*, vol. 50A, pages 67 – 74, 2004.

[10] A. Ghosh, K. Robbins, and W. Sampson, "Magnetization measurements on multifilamentary Nb_3Sn and NbTi conductors", *IEEE Trans. Magn.*, vol. 21, Issue 2, Pages 328 – 331, Mar. 1985.